

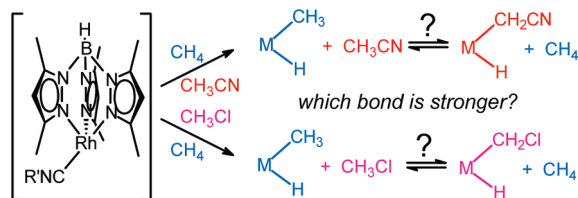
Thermodynamic Trends in Carbon–Hydrogen Bond Activation in Nitriles and Chloroalkanes at Rhodium

Meagan E. Evans, Ting Li, Andrew J. Vetter, Ryan D. Rieth, and William D. Jones*

Department of Chemistry, University of Rochester, Rochester, New York 14627

jones@chem.rochester.edu

Received June 9, 2009



Several transition-metal systems have been used to establish correlations between metal–carbon and carbon–hydrogen bonds. Here, the $[Tp'RhL]$ fragment, where Tp' = tris(3,5-dimethylpyrazolyl)borate and L = neopentyl isocyanide, is used to investigate C–H bond activation in a series of linear alkylnitriles and chloroalkanes. Using a combination of kinetic techniques, relative free energies can be found for the compounds $TpRhL(CH_3)H$, $Tp'RhL[(CH_2)_nCN]H$ ($n = 1-5$), and $Tp'RhL[(CH_2)_mCl]H$ ($m = 1, 3, 4, 5$). It is found that the CN and Cl substituents dramatically strengthen the M–C bond more than anticipated if in the α -position, with the effect on bond strength diminishing substantially as the X group moves further from the metal (i.e., β , γ , δ). Examination of M–C vs C–H bond strengths shows that the $Tp'RhL(CH_2X)H$ compounds ($X = \text{phenyl, vinyl, CN, Cl}$) all show a good correlation, as do the alkyl, aryl, and vinyl derivatives. The compounds in the former group, however, have stronger M–C bonds than expected based on the C–H bond strengths and consequently, their correlation is separate from the other unsubstituted compounds.

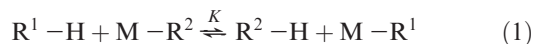
Introduction

The activation of strong C–H bonds by transition-metal complexes allows for an entry into organometallic complexes that can be subsequently transformed to produce new organic derivatives. While substantial progress has been made in developing these functionalization reactions, control of the selectivity, i.e., which C–H bond undergoes cleavage, is critical in limiting the distribution of products to a single desired compound. In understanding how to control selectivity, detailed knowledge of metal–carbon bond strengths and the factors that affect these strengths is critical to designing selective routes to products. The interplay of kinetics and thermodynamics is also centered on the strengths of bonds that are being broken and formed, so studies of this nature provide a fundamental basis for making predications regarding reactivity.

Absolute measurements of metal–carbon bond strengths are difficult and limited to cases where thermochemical measurements have proven easy or possible to perform.^{1–3}

In contrast, relative bond strengths can be obtained by examination of equilibria between various substrates that can be activated reversibly, such as occurs in oxidative addition/reductive elimination reactions of X–H bonds. In these equilibrations, one is comparing both the strength of the X–H bond being broken and the strength of the M–X bond being formed, such that the combined difference is what determines the position of the equilibrium. For example, eq 1 shows equilibration of two different R–H substrates for oxidative addition to a metal center M. The reaction can be driven to the right by a strong M–R¹ bond *and* by a weak R¹–H bond, whereas it can be driven to the left by a strong M–R² bond *and* by a weak R²–H bond. If one assumes that the entropy change in this type of reaction is near zero, then the equilibrium constant K can be converted to a free energy ΔG which approximates the enthalpy change for the reaction (ΔH), as indicated in eq 2. Since many substrate R–H bond strengths are known, this equation can be rearranged and combined with the equilibrium constant to provide a way to determine relative M–R

bond strengths, as indicated in eq 3.



$$\Delta H = D_{R^1-H} + D_{M-R^2} - (D_{R^2-H} + D_{M-R^1}) \quad (2)$$

$$(D_{M-R^2} - D_{M-R^1}) = -RT \ln(K) - D_{R^1-H} + D_{R^2-H} \quad (3)$$

One of the first general studies of this type to be performed is the report by Bryndza and Bercaw in which relative metal-hydrogen, -oxygen, -nitrogen, and -carbon bond strengths were determined in both organoruthenium and organoplatinum compounds using equilibrium studies with Cp* (PM₃)₂-RuX (Cp* = C₅Me₅), and (dppe)MePtX (dppe = 1,2-bis(diphenylphosphino)ethane).⁴ Data for Cp*₂Sc-X, Cp*₂(OCMe₃)Th-X, and Cp*(PM₃)₂(H)Ir-X were also compared. Examination of the relative M-X bond energies with the corresponding H-X bond energies showed a good correlation for most substrates with a slope of 1 (Figure 1), indicating that the strength of the bond being made was balanced by the strength of the bond being broken. It should be noted that some of the comparisons between the metal complexes were made by assuming values for the M-X bond strengths.

Another case where a series of metal-carbon bond strengths could be compared is in the (t-Bu₃SiO)₂(t-Bu₃SiNH)TiR series of complexes studied by Wolczanski.^{5,6} Approximately 15 different alkyl, aryl, benzyl, and vinyl M-R derivatives were equilibrated with each other, allowing a ladder of relative energies to be established. A good correlation between M-C and H-C bond strengths was observed, giving a line with a slope of 1.1, indicating that differences in M-C bond strengths were about 10% greater than differences in H-C bond strengths

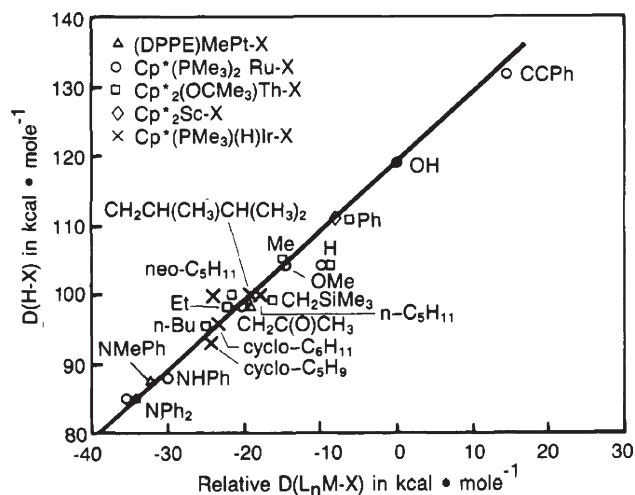


FIGURE 1. Cumulative plot of H-X vs relative L_nM-X bond strengths discussed in ref 4. Data for (dppe)MePt-X (Δ), Cp*(PM₃)₂Ru-X (○), Cp*₂Sc-X (◇), Cp*₂(OCMe₃)Th-X (□), and Cp*(PM₃)₂(H)Ir-X (×) depicted for X = singly bonded first-row main group substituents along with the arbitrary line (slope = 1.00; intercept = 119.0 kcal mol⁻¹). Scale definitions for (dppe)MePtX, Cp*(PM₃)₂Ru-X, and Cp*₂(OCMe₃)Th-X data as described in ref 4. To put the Sc-X data on these axes the Sc-C bond in Cp*₂Sc-Ph has been defined as -8.1 kcal mol⁻¹; similarly, the Ir-C bond in Cp*(PM₃)₂(H)Ir-cyclo-C₆H₁₁ has been assigned an arbitrary value of -21 kcal mol⁻¹. A good 1:1 correlation of H-X and M-X bond strengths is noted.

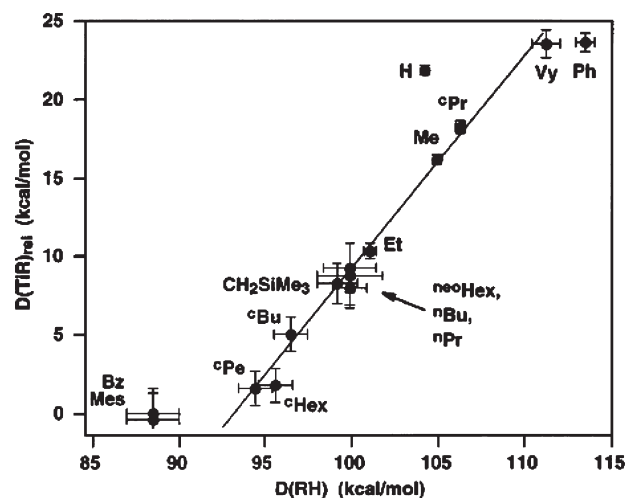


FIGURE 2. Relative Ti-C bond strengths (kcal/mol) in (silox)₂(t-Bu₃SiNH)TiR versus the C-H bond strength of the corresponding hydrocarbon from ref 6. $D(\text{TiR})_{\text{rel}} = D(\text{TiR}) - D(\text{TiBz})$, with $\Delta H^{\circ}_{\text{reacn}}$ estimated from $\Delta G^{\circ}_{\text{corr}}$. The line (slope = 1.36, $r = 0.9953$) is a least-squares fit to the points except Bz, Mes, H, and Ph. A least-squares line to all points had a slope of 1.1 ($r = 0.95$).

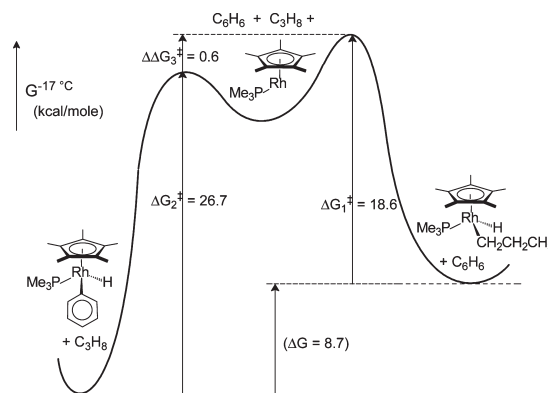


FIGURE 3. Relationship between kinetic measurements made to determine ΔG for the reaction: $M(R_1)H + R_2-H \rightleftharpoons M(R_2)H + R_1-H$, where $R_1 = \text{Ph}$ and $R_2 = n\text{-propyl}$. Based on ref 10.

(Figure 2). A related study with (t-Bu₃SiNH)₂(t-Bu₃-SiN=)TaR complexes (R = Ph, Me, benzyl) led to a M-C/H-C correlation with a slope of 1.0, indicating a 1:1 trade-off between bond strengths for this system,⁷ as seen in the Bryndza/Bercaw studies. Similarly, examination of R-H exchange reactions in (t-Bu₃SiNH)₃ZrR complexes led to the conclusion that differences in M-C and H-C bond strengths canceled each other in a 1:1 fashion, leading to equilibrium constants near 1 for these derivatives also.⁸

Our group's interest in the thermodynamics of C-H bond activation dates back to the early 1980s when we discovered that the fragment [Cp*Rh(PMe₃)] could activate both aromatic and aliphatic C-H bonds via oxidative addition.⁹ In the case of this metal fragment, however, the equilibrium laid so heavily in favor of benzene activation that simple equilibration with an alkane was not possible. We developed a kinetic method to assess equilibrium constants, or more correctly, free energies for hydrocarbon exchange reactions as indicated in Figure 3 for the case of benzene vs propane

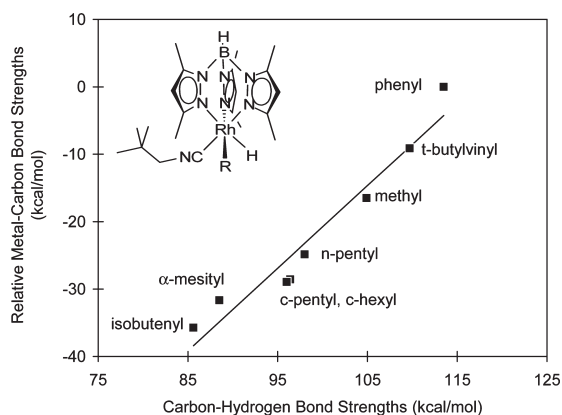


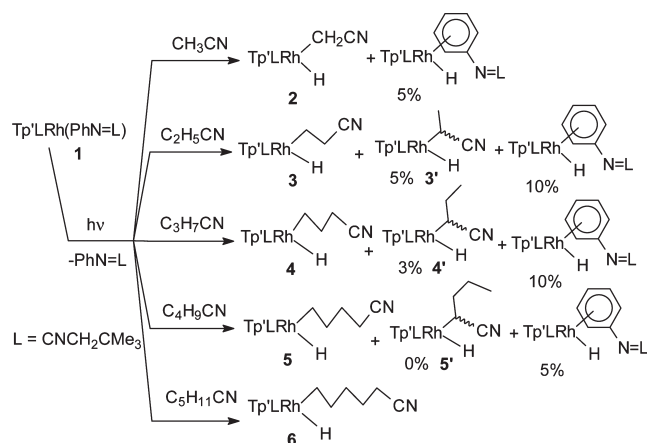
FIGURE 4. Plot of relative metal–carbon bond strengths in $\text{Tp}'\text{RhL}(\text{R})\text{H}$ compounds vs the corresponding C–H bond strengths from ref 13. The slope of the line is 1.22.

activation.¹⁰ Three experiments are needed to determine the free energy difference for the exchange. The first two involve measurement of the rate of reductive elimination of the hydrocarbon, which can then be used in the Eyring equation to produce the corresponding barrier heights for the elimination (ΔG^\ddagger). Then, a competition experiment is run by producing the metal fragment (photochemically) in a mixture of the two substrates under conditions where the products are stable (-20°C), allowing an evaluation of the difference in the two C–H activation barrier heights ($\Delta\Delta G^\ddagger$). The combination of these three activation energies then produces a value for ΔG for the equilibrium which is then used in eq 3 to obtain relative metal–carbon bond strengths. This system was the first to suggest that the metal–aryl bond was much stronger than the metal–alkyl bond, by ~ 21 kcal/mol, which is much larger than the difference in the C–H bonds being broken ($112.9 - 100.9 = 12$ kcal/mol)!¹¹ Also, this conclusion stands in strong contrast to the conclusions seen by Wolczanski and Bryndza and Bercaw in their later work.

Additional support for the notion that the difference in metal–carbon bond strengths can be greater than the difference in carbon–hydrogen bond strengths came from a series of investigations of C–H oxidative addition reactions of the fragment $[\text{Tp}'\text{RhL}]$ where $\text{Tp}' = 3,5\text{-dimethyltrispyrazolyl borate}$ and $\text{L} = \text{neopentyl isocyanide}$. This fragment activates a wide variety of hydrocarbon C–H bonds, including aromatic, aliphatic, vinylic, and benzylic.¹² Using the above-mentioned kinetic technique for measuring ΔG values for hydrocarbon exchange reactions, a series of bond strengths could be determined and a correlation made with C–H bond strengths, as indicated in Figure 4. The slope of the best-fit line is 1.22, which means that the difference in Rh–C bond strengths are generally 20% greater than the difference in C–H bond strengths. The apparent “curvature” of the data was noted earlier, although no explanation could be provided.¹³

In this paper, we provide additional analysis of the factors that influence metal–carbon bond energies. Specifically, we will examine the effect that nitrile and chlorine substituents have on metal–carbon bond strengths. We will show that substituents on carbon α to a metal center can dramatically affect bond strengths in a way that is surprising and un-

SCHEME 1. Summary of C–H Activation of Nitriles



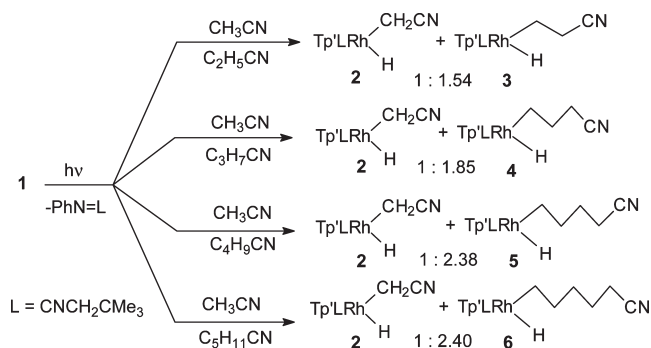
expected and provide a quantitative evaluation of this effect. We will also provide insight into the “curvature” in the above-mentioned plot.

Results and Discussion

C–H Activation of Nitriles. We reported previously that generation of the fragment $[\text{Tp}'\text{RhL}]$ ($\text{L} = \text{neopentyl isocyanide}$) by photolysis of $\text{Tp}'\text{RhL}(\text{carbodiimide})$ **1** in acetonitrile solvent leads to the clean activation of the nitrile C–H bond, giving $\text{Tp}'\text{RhL}(\text{CH}_2\text{CN})\text{H}$, **2** (Scheme 1).¹⁴ This octahedral complex has C_1 symmetry, and its NMR spectroscopic data is consistent with this geometry, displaying two resonances for the diastereotopic methylene hydrogens in the ^1H NMR spectrum and a hydride resonance with $J_{\text{Rh-H}}$ of only 20 Hz (all other $\text{Tp}'\text{RhL}(\text{R})\text{H}$ compounds display $J_{\text{Rh-H}} = 24\text{--}25$ Hz). The molecule is remarkably stable in that it has a half-life for reductive elimination of acetonitrile of 3.7 days at 100°C in benzene. In comparison, the unsubstituted methyl hydride complex $\text{Tp}'\text{RhL}(\text{CH}_3)\text{H}$ has a half-life for methane reductive elimination of only ~ 4 h at ambient temperature. Consequently, the replacement of a hydrogen by a cyanide on the α -carbon apparently strengthens the metal–carbon bond tremendously, resulting in the observed increase in stability. Upon reflection of this conclusion, however, it seemed that just the opposite effect should have been observed. That is, the $\text{Rh-CH}_2\text{CN}$ bond should be *weaker* than the Rh-CH_3 bond, since the radical formed ($^{\bullet}\text{CH}_2\text{CN}$, $D_{\text{C-H}} = 94.8$ kcal/mol¹⁵) is more stable than the methyl radical ($^{\bullet}\text{CH}_3$, $D_{\text{C-H}} = 105.0$ kcal/mol¹¹). We'll return to this puzzling dilemma after consideration of the behavior of other nitriles.

Propionitrile reacts with the $[\text{Tp}'\text{Rh}(\text{L})]$ fragment to give a C–H activation product in which the terminal methyl group has undergone oxidative addition as the major species. Due to the stabilizing effect of an α -cyano group seen with acetonitrile, it might have been expected to observe the branched compound **3'** as the major product, but only $\sim 5\%$ of this species was seen. As expected, **3'** has a reduced coupling constant for its hydride resonance ($J_{\text{Rh-H}} = 20$ Hz) compared to **3** ($J_{\text{Rh-H}} = 24$ Hz). In addition, small quantities of *o*-, *m*-, and *p*-aryl hydride activation products of the released carbodiimide can be detected. At 26°C , **3** has a half-life for reductive elimination of 128 h, substantially longer than its ethyl hydride counterpart $\text{Tp}'\text{RhL}(\text{Et})\text{H}$ (63 min¹⁶).

SCHEME 2. Nitrile Competition Studies



As anticipated, the branched product **3'** has a much longer lifetime and persists for days, even upon heating.

Similar behavior was seen with butyronitrile. The dominant product was the linear methyl C–H activation product **4** with only 3% of the branched α -cyano product **4'** seen, along with small quantities of the carbodiimide activation byproducts. Once again, the hydride coupling constant for **4'** was smaller ($J_{\text{Rh-H}} = 20$ Hz) compared to that of **4** ($J_{\text{Rh-H}} = 24$ Hz). The lifetime for reductive elimination of butyronitrile from **4** was 5.9 h, compared with 44 min for $\text{Tp}'\text{RhL}(n\text{-propyl})\text{H}$. **4'** persisted for several days, even upon heating.

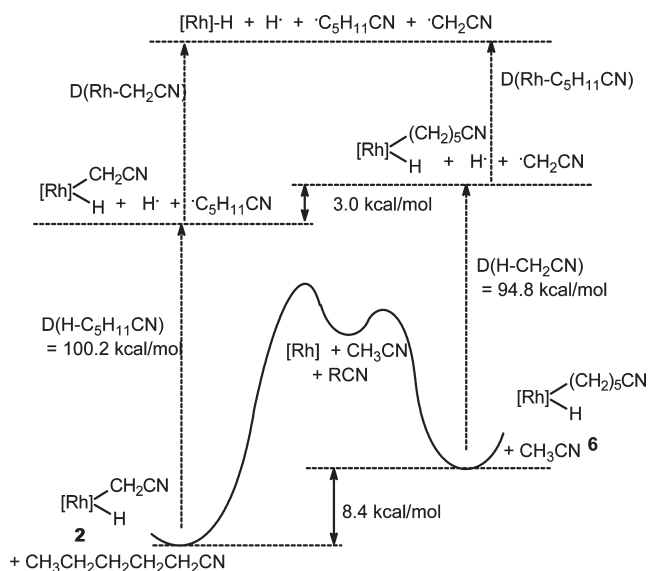
The activation of valeronitrile by photolysis of a solution containing **1** was even cleaner, producing terminal activation product **5** but no detectable branched product **5'**. Only traces of the carbodiimide arene activation products were seen. At 26 °C, the half-life of **5** was 1.6 h, compared to a half-life of 42 min¹⁶ for the parent compound $\text{Tp}'\text{RhL}(n\text{-butyl})\text{H}$. The effect of the cyano substituent can therefore be noticeable even 4-carbons removed from the metal center! Activation of capronitrile gives only the terminal C–H activation product **6**. The half-life for reductive elimination of nitrile in benzene at 26 °C is comparable ($\tau = 48$ min) to the rate of pentane loss from $\text{Tp}'\text{RhL}(n\text{-pentyl})\text{H}$ ($\tau = 43$ min¹⁶).

With these reductive elimination barriers in hand, we realized that competition experiments of one nitrile vs another could allow us to establish the relative energetics of the Rh–C bonds in these nitrile-substituted derivatives, just as we had done previously for the hydrocarbons. Consequently, equimolar solutions of acetonitrile and each of the longer chain nitriles ($\text{C}_1\text{--}\text{C}_5$) containing **1** were photolyzed, and the kinetic C–H product distributions were obtained (Scheme 2). From these kinetic product selectivities, the relative barrier heights could be determined, and combined with the reductive elimination barriers, the ΔG values and equilibrium constants could be determined as indicated in Table 1. In all equilibrations, acetonitrile adduct **2** is the most stable complex but is kinetically the least preferred compared to the longer chain nitriles. This has been interpreted in terms of rate-determining binding to the C–H groups in the nitrile to give an alkane σ -complex,¹⁷ followed by migration down the chain to the methyl group, where C–H insertion occurs.¹⁴ In fact, these competition selectivities have been predicted reasonably well¹⁴ using kinetic simulations with rate constants obtained for alkane binding¹⁸ and activation.¹⁶ From the data in Table 1, the ΔG can be seen to be leveling off at about 8 kcal/mol for the longer chain nitriles.

TABLE 1. Reductive Elimination Barriers, Competitive Barriers, and Free Energies for $\text{Tp}'\text{RhL}[(\text{CH}_2)_n\text{CN}]\text{H}$ Complexes

complex	RCN	k_{rel}^a	$\Delta G_{\text{re}}^\ddagger$	$\Delta\Delta G_{\text{oa}}^\ddagger$	ΔG
2	CH_3CN	6×10^5	31.36	0	0
3	$\text{C}_2\text{H}_5\text{CN}$	121	25.47	0.22	5.67
4	$\text{C}_3\text{H}_7\text{CN}$	8.1	23.64	0.31	7.41
5	$\text{C}_4\text{H}_9\text{CN}$	2.3	22.88	0.44	8.04
6	$\text{C}_5\text{H}_{11}\text{CN}$	1.1	22.48	0.52	8.36

$$^a k_{\text{rel}} = (k_{\text{obs}}, \text{R}^{\text{H}})/(k_{\text{obs}}, \text{R}^{\text{CN}})$$

FIGURE 5. Comparison of Rh–CH₂CN and Rh–CH₂CH₂CH₂CH₂CH₂CN bond energies.

At this point, a useful construction can be made to compare bond energies in these compounds. As shown in Figure 5, comparison of the acetonitrile activation and capronitrile activation reactions can be made if we include two additional steps: (1) break the C–H bond of the substrate and (2) break the Rh–R bond of the metal complex. It can be seen that these upper two processes correspond to rupture of the Rh–C bond and that their difference can be calculated to be 3 kcal/mol favoring a stronger Rh–CH₂CN bond compared to a Rh–CH₂CH₂CH₂CH₂CH₂CN bond. Therefore, the cyanomethyl bond is indeed a strong M–C bond. But does this make sense? In terms of stability, the ϵ -capronitrile radical is essentially the same as that for an n -pentyl radical ($D_{\text{C-H}} = 100.2$ kcal/mol¹¹) and should be much more difficult to form than the cyanomethyl radical ($D_{\text{C-H}} = 94.8$ kcal/mol¹⁵).

In further consideration of this problem, it became clear that what should really be compared is the effect of cyano substitution with the methyl complex $\text{Tp}'\text{RhL}(\text{CH}_3)\text{H}$, not the ϵ -capronitrile complex **6**. But how could this be accomplished experimentally since a competition between methane and acetonitrile would not be possible (alkanes are immiscible with acetonitrile)? We were able to circumvent this issue by performing a competition between pentane and capronitrile, which are miscible, which showed a 1.7:1 kinetic preference for pentane activation. This allows comparison of the energy of cyanomethyl product **2** and the n -pentyl complex $\text{Tp}'\text{RhL}(n\text{-pentyl})\text{H}$, as shown in Figure 6. Furthermore, we can establish the relative energetics of the complexes

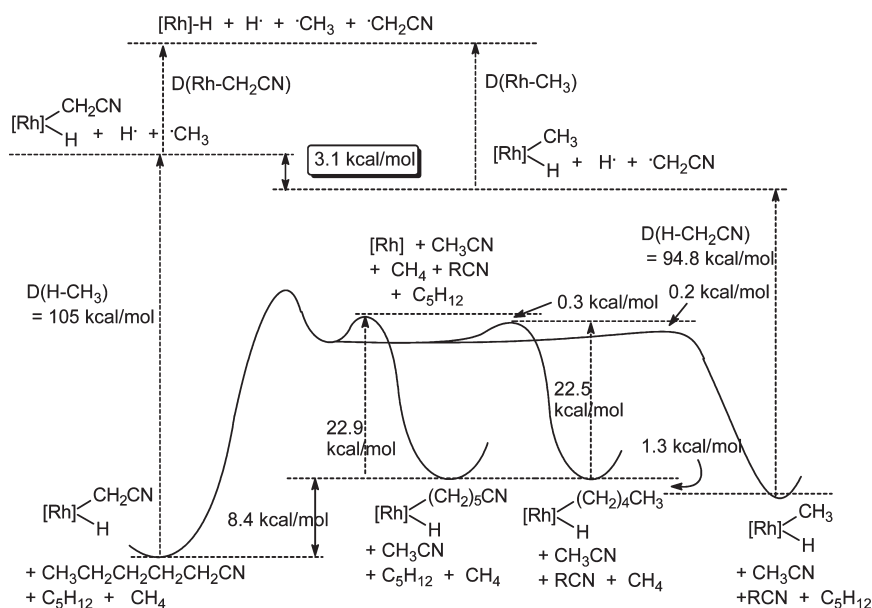
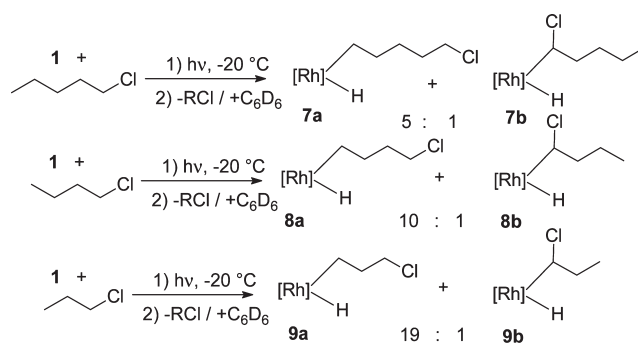


FIGURE 6. Comparison of the energies of cyanomethyl and methyl derivatives of $\text{Tp}'\text{RhL}(\text{R})\text{H}$.

$\text{Tp}'\text{RhL}(n\text{-pentyl})\text{H}$ and $\text{Tp}'\text{RhL}(\text{CH}_3)\text{H}$ using their reductive elimination rates and by performing a competition between methane and pentane (the latter shows a 1.4: 1 kinetic preference for methane). These two additional steps can be combined with the result that the energies of the cyanomethyl complex **2** can be compared directly with the methyl complex $\text{Tp}'\text{RhL}(\text{CH}_3)\text{H}$. Once again, inclusion of the C–H bond energies allows us to obtain the difference in the strength of the rhodium–methyl and rhodium–cyanomethyl bonds (Figure 6). As can be seen in Figure 6, the Rh–methyl bond is about 3 kcal/mol stronger than the Rh–cyanomethyl bond. This makes sense based on the relative stabilities of the carbon-based radicals formed by Rh–C homolysis. What is interesting is that the difference in Rh–C bond strengths (3 kcal/mol) is smaller than the difference in C–H bond strengths (10 kcal/mol); that is, the Rh–cyanomethyl bond is about 7 kcal/mol stronger than one would “expect” it to be on the basis of C–H bond strengths. What could be the origin of this additional stability? The most obvious difference is that the cyano group stabilizes negative charge on the α -carbon, and thereby increases the ionic component of the Rh–C bond. Ionic bonds are stronger than covalent bonds, so this results in an increase in bond strength with cyano substitution. The same effect applies, although to a lesser extent, to the longer chain nitriles. As the cyano group moves away from the metal (β , γ , δ , etc.), the ability to stabilize negative charge on the α -carbon diminishes (for CN, $\sigma_1 = 0.51$; for CH_2CN , $\sigma_1 = 0.32$; for $\text{CH}_2\text{CH}_2\text{CN}$, $\sigma_1 = 0.09$),¹⁹ and the bond strength approaches that of a “normal” alkyl complex. The ability to stabilize negative charge on the α -carbon has recently been invoked and demonstrated with DFT calculations to explain the *o*-fluorine effect on stabilizing metal–aryl bonds.²⁰ It is also worth noting that the equilibration of $[\text{M}]\text{--CH}_2\text{CH}_2\text{CN}$ and $[\text{M}]\text{--CH}(\text{CN})\text{CH}_3$ where $[\text{M}] = [\text{CpFe}(\text{CO})(\text{PPh}_3)]$ or $[(\text{Me}_2\text{NCS}_2)\text{Pd}(\text{PET}_3)]$ has been observed to favor the latter, probably for the same reasons as outlined here.²¹

C–H Activation of Chloroalkanes. Alkyl halides are well-known to undergo oxidative addition of the C–X bond with

SCHEME 3. Irradiation of $\text{Tp}'\text{RhL}(\text{carbodiimide})$ with Chloroalkanes



Rh^{I} and Ir^{I} complexes,^{22,23} which is why it was surprising to find that irradiation of **1** in 1-chloropentane led to a strong preference for terminal methyl C–H activation to give **7a** (Scheme 3).²⁴ No evidence for C–Cl addition was seen, even though $\text{Tp}'\text{RhL}(n\text{-pentyl})\text{Cl}$ is known to be a stable complex.¹² Small quantities of $\text{Tp}'\text{RhLHCl}$ were also formed (8%), however, presumably arising from C–H activation of a secondary C–H bond β to the chlorine followed by rapid β -chloro elimination. (Irradiation of **1** in 2-chloropropane gives exclusively propene and $\text{Tp}'\text{RhLHCl}$.) In addition, evidence was seen for a small amount of activation of the α -chloro C–H bond (13%), just as seen with the nitriles. This species **7b** shows two characteristic features in common with the α -cyano alkyl hydride complexes: (1) it has a long lifetime toward reductive elimination of chloropentane, and (2) it displays a reduced Rh–H coupling constant for hydride resonance ($J_{\text{Rh-H}} = 20$ Hz).

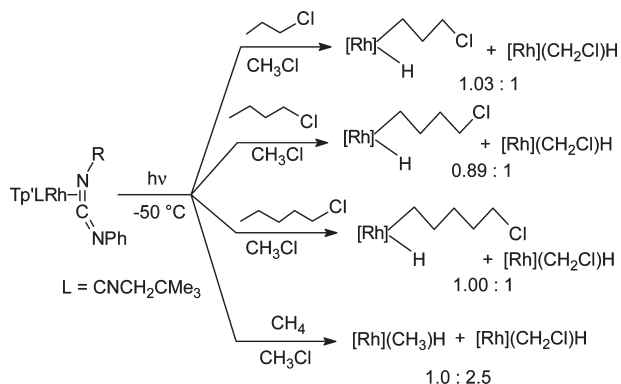
Similar results were observed with 1-chloropropane and 1-chlorobutane.²⁵ In these substrates, however, more terminal activation product was obtained (**8a** or **9a**) with a shorter alkyl chain. These results were interpreted in terms of a more rapid migration down to the end of the chain, followed by C–H activation, with the shorter alkyl chloride.

TABLE 2. Relative Rates for Reductive Elimination from $\text{Tp}'\text{Rh}(\text{L})(\text{R}^{\text{Cl}})\text{H}^{25}$ and $\text{Tp}'\text{Rh}(\text{L})(\text{R}^{\text{H}})\text{H}^{16}$ in C_6D_6

$\text{R}^{\text{Cl}}/\text{R}^{\text{H}}$	T ($^{\circ}\text{C}$)	$k_{\text{obs}}, \text{R}^{\text{Cl}}, \text{s}^{-1}$	$k_{\text{obs}}, \text{R}^{\text{H}}, \text{s}^{-1}$	k_{rel}^b	ΔG^\ddagger , kcal/mol
CH_2Cl	80	$\sim 4 \times 10^{-5}$			~ 27.9
$\text{CH}_2\text{Cl}/\text{CH}_3$	26	$\sim 3 \times 10^{-8}$ ^a	$4.51(3) \times 10^{-5}$	~ 2000	~ 27.9
$\text{CH}_2\text{CH}_2\text{Cl}/\text{Et}$	26	$\beta\text{-Cl}$ eliminates	$1.82(7) \times 10^{-4}$		
$\text{CH}_2\text{CH}_2\text{CH}_2\text{Cl}/\text{Pr}$	26	$4.21(3) \times 10^{-5}$	$2.63(7) \times 10^{-4}$	6.3	23.49
$\text{CH}_2\text{CH}_2\text{CH}_2\text{CH}_2\text{Cl}/\text{Bu}$	26	$1.12(1) \times 10^{-4}$	$2.77(14) \times 10^{-4}$	2.5	22.91
$\text{CH}_2\text{CH}_2\text{CH}_2\text{CH}_2\text{CH}_2\text{Cl}/\text{Pn}$	26	$1.80(5) \times 10^{-4}$	$2.70(8) \times 10^{-4}$	1.5	22.63

^aEstimated assuming ΔG^\ddagger is temperature independent over this range. ^b $k_{\text{rel}} = (k_{\text{obs}}, \text{R}^{\text{H}})/(k_{\text{obs}}, \text{R}^{\text{Cl}})$.

SCHEME 4. Chloroalkane Competition Reactions



Irradiation of **1** in liquid chloromethane at -20 $^{\circ}\text{C}$ results in the formation of $\text{Tp}'\text{RhL}(\text{CH}_2\text{Cl})\text{H}$ in 80% yield. This product shows a low Rh–H coupling for the hydride ligand ($J_{\text{Rh-H}} = 20$ Hz) and decomposes slowly at 80 $^{\circ}\text{C}$ without producing CH_3Cl . Consequently, we can take this decomposition rate as the upper limit for the rate at which this complex would eliminate chloromethane.

The rates of reductive elimination of chloroalkane from **7a**, **8a**, and **9a** were found to be slower than in their unsubstituted parent alkyl hydride complexes. As indicated in Table 2, the relative first-order rate constants for reductive elimination are several times faster for the alkane than for the corresponding chloroalkane, again showing the effect of an electronegative group on increasing the M–C bond strength. Also shown in Table 2 is the approximate value for reductive elimination of chloromethane.

The barriers for reductive elimination can also be determined from these rate constants. As done with acetonitrile, competitive activation reactions were undertaken to allow for a comparison of the Rh–C bond strengths in these reactions. Scheme 4 shows the results, which differ distinctly from the nitrile competitions. In competitions between two chloroalkanes, a 1:1 product distribution is seen for **7a**, **8a**, and **9a** vs $\text{Tp}'\text{RhL}(\text{CH}_2\text{Cl})\text{H}$. This observation indicates that all chloroalkanes react at the same rate, and has been interpreted in terms of rate determining coordination of the metal to the chlorine, followed by rapid migration down the chain and insertion into the methyl C–H bond.²⁵ Support for this hypothesis comes from the competition between methane and chloromethane, where it is observed that the chloroalkane is substantially more reactive with the rhodium fragment than the alkane.

Finally, a thermodynamic analysis of the Rh–C bond strengths can be made as done with the nitriles. Figure 7 shows a comparison of methane and chloromethane C–H activations (the initially formed $\sigma\text{-CH}_4$ and $\sigma\text{-ClCH}_3$ adducts

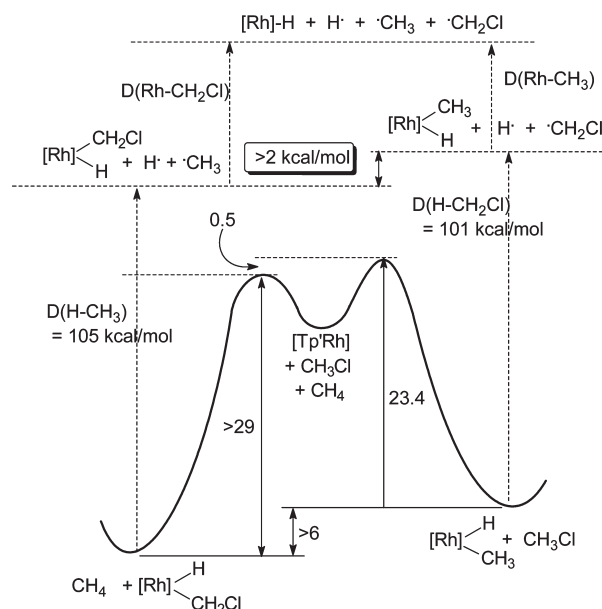


FIGURE 7. Analysis of rhodium–methyl and rhodium–chloromethyl bond strengths.

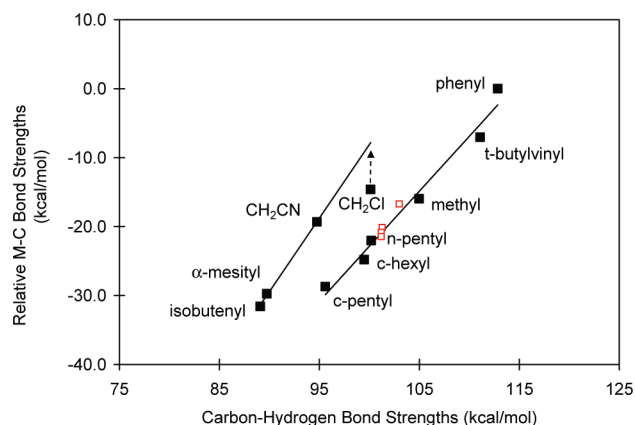


FIGURE 8. Comparison of rhodium–carbon and hydrogen–carbon bond strengths. The slopes of the upper and lower lines are 2.13 and 1.59, respectively. The data shown in four open red squares are for propionitrile, butyronitrile, valeronitrile, and capronitrile, top to bottom, using DFT calculated C–H bond strengths.

are not shown). We have established that the barrier for methane activation is slightly higher than for chloromethane activation, and we know the barrier for methane reductive elimination. A lower limit of 29 kcal/mol can be placed on the barrier to chloromethane elimination from $\text{Tp}'\text{RhL}(\text{CH}_2\text{Cl})\text{H}$, which indicates that the latter is

TABLE 3. Calculated and Experimental C–H Bond Strengths in Linear Nitriles and Hydrocarbons

substrate	radical	D_{C-H} calcd (exptl), kcal/mol
CH ₃ CN	•CH ₂ CN	93.3 (94.8)
CH ₃ CH ₂ CN	•CH ₂ CH ₂ CN	103.0
CH ₃ CH ₂ CH ₂ CN	•CH ₂ CH ₂ CH ₂ CN	101.3
CH ₃ CH ₂ CH ₂ CH ₂ CN	•CH ₂ CH ₂ CH ₂ CH ₂ CN	101.2
CH ₃ CH ₂ CH ₂ CH ₂ CH ₂ CN	•CH ₂ CH ₂ CH ₂ CH ₂ CH ₂ CN	101.2
CH ₃ CH ₂ CH ₂ CH ₂ CH ₃	•CH ₂ CH ₂ CH ₂ CH ₂ CH ₃	101.3 (100.2)

preferred thermodynamically by at least 6 kcal/mol over Tp'RhL(CH₃)H. Combining this ΔG with the methane¹¹ and chloromethane²⁶ C–H bond strengths leads to the conclusion that the rhodium–chloromethyl bond is at least 2 kcal/mol stronger than the rhodium–methyl bond, since the barrier to reductive elimination is likely 1–2 kcal/mol higher than indicated in Table 2. As seen with nitriles, the α -chloro group also strengthens the rhodium–carbon bond significantly compared to what one would expect based on C–H bond strengths, but not as much as a cyano group. This can also be seen in the reduced inductive effect that chloro substitution has on reductive elimination rates compared to the nitriles; i.e., the range of k_{rel} values in Table 2 is reduced compared to Table 1.

Thermodynamics of C–H Activation. A quantitative analysis of these new revelations about α -substituents on rhodium–carbon bond strengths can be seen if these data are added to the graph in Figure 4, as shown in Figure 8. The first obvious difference is that the data appear to fit better to two distinct lines. One line best describes the behavior of R groups where the anion is stabilized through resonance and/or inductive effects (e.g., benzylic, allylic). The other line fits the “normal” hydrocarbons where resonance stabilization of the anion is absent. Chloromethyl lies above the alkyl line as the chlorine does stabilize negative charge on the α -carbon but may not quite reach the line for the α -stabilized R groups since no resonance stabilization of the anion is present. This also may be because while the C–H bond is weaker in chloromethane than in methane, it is not nearly as weak as the C–H bond in acetonitrile. The slopes of the two lines are almost identical, suggesting that there is an additive effect of the ionic supplement to the increase in M–C bond strength. If one uses the enthalpy values for the linear nitriles (propionitrile–capronitrile) and calculates the terminal methyl C–H bond strengths in these molecules using DFT, these species can be seen to lie very close to the line for the “normal” hydrocarbons (Figure 8, red squares).

Conclusions

In this paper, we have reviewed trends in M–C bond strengths and shown that for the [Tp'RhL] fragment (L = neopentyl isocyanide), there appear to be two classes of metal–carbon bonds. One class comprises “ordinary” M–R bonds in which the R group has no special resonance or inductive stabilization of negative charge on carbon. A second class is observed for M–R bonds in which the R group is capable of stabilizing negative charge through resonance and/or inductive effects. These same R groups have weak C–H bonds again due to stabilization of the radical that is formed as a result of the substituent on the α -carbon. The differences in M–C bond strengths in this system are about 60% greater than differences in H–C bond

strengths within the unsubstituted substrates but rise to over 100% for the α -substituted methyl substrates. Curiously, compounds with weaker M–C bonds due to the presence of an α -substituent appear to have greater “stability” than the parent methyl derivative, as the kinetic barrier to reductive elimination is larger for these derivatives than for the methyl hydride complex. This effect is attributed to an increase in ionic character of the M–C bond.

Experimental Section

The bulk of the kinetic and competition experiments described here were reported in refs 14 and 25. The additional experiments mentioned below were added to these studies to permit the analysis that is presented here. Note that the competition between pentane and methane was assumed to be 1:2 in ref 12 but now has been measured to be 1:1.4.

Activation/Elimination of Capronitrile. Compound **1** (6 mg) was placed in a resealable NMR tube. Roughly 0.1 mL of capronitrile was added. The resulting dark yellow solution was kept at -20 °C and photolyzed for 20 min. The solution was diluted with 0.5 mL of C₆D₆, and 0.5 μ L of an internal standard (hexamethyldisiloxane) was added. The resulting solution was placed in a 26 °C NMR probe and monitored by ¹H NMR spectroscopy over the course of 4 h. The spectra obtained showed the disappearance of the C–H activation product and were used to determine the rate of reductive elimination, $2.41(12) \times 10^{-4} \text{ s}^{-1}$. Data and plots are shown in the Supporting Information.

Competition of CH₃CN and Capronitrile. Compound **1** (6 mg) was placed in a resealable NMR tube and was treated with 0.20 mL of pentane and 0.20 mL capronitrile. The sample was irradiated at -20 °C for 20 min and analyzed by ¹H NMR spectroscopy immediately after excess substrate was removed in vacuo, and the remaining residue was dissolved in C₆D₆. The ratio of the resulting hydrides from activation of CH₃CN (δ –14.34) vs 1-cyanopentane (δ –14.94) was measured and corrected based on the molar ratio of substrates present in the sample before photolysis, showing a 2.4:1 preference for capronitrile product **6**. Spectra are shown in the Supporting Information.

Competitive Activation of Pentane and Methane. A high-pressure NMR tube was charged with 5 mg of **1** dissolved in 0.3 mL of C₆D₁₂ and pentane (20 μ L) added. The sample was freeze–pump–thaw degassed, and methane was added to the tube (charged tube with 30 psi). The tube was shaken vigorously for 10 min, after which time it was irradiated at room temperature for 10 min, and a ¹H NMR spectrum was recorded immediately. The ratio of the resulting hydrides from activation of pentane and from activation of methane was measured. The product ratio was corrected for the initial concentrations of the two reactants in solution based on integration of their ¹H NMR resonances, resulting in a 1.4:1 preference for methane activation over pentane on a per molecule basis. Spectra are shown in the Supporting Information.

Calculation of C–H Bond Strengths in Alkyl nitriles. The methyl C–H bond strengths in the linear alkyl nitriles were

calculated using DFT (B3LYP/6-31G**) as indicated in Table 3.²⁷ Note that other than for acetonitrile, these values cannot be measured experimentally as the α -cyano C–H bonds are the weakest and therefore the first to undergo abstraction in a homolytic (radical) reaction. The enthalpies of the nitriles were compared with the enthalpies of the corresponding radical fragments ($\text{H}^\bullet + \text{NC}(\text{CH}_2)_n\text{CH}_2^\bullet$) to obtain the bond strengths. The absolute value calculated of the C–H bond strength for capronitrile is very close to both the calculated and experimental value in pentane, indicating good agreement between this method and experiment. These calculated bond strengths were used in the plot shown in Figure 8 for the alkylnitriles propionitrile–capronitrile.

Acknowledgment. We acknowledge the U.S. Department of Energy Office of Basic Energy Sciences for their support of this work (Grant No. FG02-86ER13569). WDJ also thanks Simon Jones for preparation of the graphic cover art associated with this Perspective.

Supporting Information Available: Table of bond energies, selectivities, and free energies used in Figure 8, a table comparing C–H bond energy calculations for the linear nitriles, NMR spectra for new competition experiments, and reductive elimination data/plots for **6**. This material is available free of charge via the Internet at <http://pubs.acs.org>.

References

- (1) Simões, J. A. M.; Beauchamp, J. L. *Chem. Rev.* **1990**, *90*, 629–688.
- (2) McDonough, J. E.; Mendiratta, A.; Curley, J. J.; Fortman, G. C.; Fantasia, S.; Cummins, C. C.; Rybak-Akimova, E. V.; Nolan, S. P.; Hoff, C. D. *Inorg. Chem.* **2008**, *47*, 2133–2141.
- (3) Scott, N. M.; Clavier, H.; Mahjoor, P.; Stevens, E. D.; Nolan, S. *Organometallics* **2008**, *27*, 3181–3186.
- (4) Bryndza, H. E.; Fong, L. K.; Paciello, R. A.; Tam, W.; Bercaw, J. E. *J. Am. Chem. Soc.* **1987**, *109*, 1444–1456.
- (5) Bennett, J. L.; Wolczanski, P. T. *J. Am. Chem. Soc.* **1994**, *116*, 2179–2180.
- (6) Bennett, J. L.; Wolczanski, P. T. *J. Am. Chem. Soc.* **1997**, *119*, 10696–10719.
- (7) Schaller, C. P.; Wolczanski, P. T. *Inorg. Chem.* **1993**, *32*, 131–144.
- (8) Schaller, C. P.; Cummins, C. C.; Wolczanski, P. T. *J. Am. Chem. Soc.* **1996**, *118*, 591–611.
- (9) Jones, W. D.; Feher, F. J. *J. Am. Chem. Soc.* **1984**, *106*, 1650–1663.
- (10) Jones, W. D.; Feher, F. J. *Acc. Chem. Res.* **1989**, *22*, 91–100.
- (11) The most recent (evaluated) hydrocarbon bond strengths are taken from: Luo, Y.-R. *Comprehensive Handbook of Chemical Bond Energies*; CRC Press: Boca Raton, 2007.
- (12) Jones, W. D.; Hessell, E. T. *J. Am. Chem. Soc.* **1993**, *115*, 554–562.
- (13) Jones, W. D.; Wick, D. D. *Organometallics* **1999**, *18*, 495–505.
- (14) Vetter, A. J.; Rieth, R. D.; Jones, W. D. *Proc. Nat. Acad. Sci. U.S.A.* **2007**, *104*, 6957–6962.
- (15) For the bond strength of CH_3CN (94.8 kcal/mol) used here, we used the heats of formation of H^\bullet (52.1 kcal/mol from *CRC Handbook of Chemistry and Physics*), $^\bullet\text{CH}_2\text{CN}$ (60.4 kcal/mol from Lafleur, R. D.; Szatary, B.; Baer, T. *J. Phys. Chem. A* **2000**, *104*, 1450–1455, and CH_3CN (17.7 kcal/mol from An, X. W.; Mansson, M. *J. Chem. Thermodyn.* **1983**, *15*, 287–293. The value listed in ref 11 states that these values were used but lists a $\text{D}(\text{H}-\text{CH}_2\text{CN})$ of 97.0 kJ/mol, which appears to be in error.
- (16) Northcutt, T. O.; Wick, D. D.; Vetter, A. J.; Jones, W. D. *J. Am. Chem. Soc.* **2001**, *123*, 7257–7270.
- (17) For DFT calculations of C–H activation via σ -complexes with this system, see: Clot, E.; Eisenstein, O.; Jones, W. D. *Proc. Nat. Acad. Sci. U.S.A.* **2007**, *104*, 6939–6944.
- (18) Vetter, A. J.; Flaschenriem, C.; Jones, W. D. *J. Am. Chem. Soc.* **2005**, *127*, 12315–12322.
- (19) Hansch, C.; Leo, A.; Taft, R. W. *Chem. Rev.* **1991**, *91*, 165–195.
- (20) Clot, E.; Mégret, C.; Eisenstein, O.; Perutz, R. N. *J. Am. Chem. Soc.* **2009**, *131*, 7817–7827.
- (21) (a) Reger, D. L.; McElligott, P. J. *J. Organomet. Chem.* **1981**, *216*, C12–C14. (b) Reger, D. L.; Garza, D. G.; Lebioda, L. *Organometallics* **1992**, *11*, 4285–4292.
- (22) Northcutt, T. O.; Lachicotte, R. J.; Jones, W. D. *Organometallics* **1998**, *14*, 5148–5152.
- (23) Collman, J. P.; Hegedus, L. S.; Norton, J. R.; Finke, R. G. *Principles and Applications of Organotransitionmetal Chemistry*; University Science Books: Sausalito, CA, 1987.
- (24) Vetter, A. J.; Jones, W. D. *Polyhedron* **2004**, *23*, 413–417.
- (25) Vetter, A. J.; Rieth, R. D.; Brennessel, W. W.; Jones, W. D. *J. Am. Chem. Soc.* **2009**, *131*, 10742–10752.
- (26) McMillen, D. F.; Golden, D. M. *Annu. Rev. Phys. Chem.* **1982**, *33*, 493–532.
- (27) For related C–H calculations, see: Henry, D. J.; Parkinson, C. J.; Mayer, P. M.; Radom, L. *J. Phys. Chem. A* **2001**, *105*, 6750–6756.